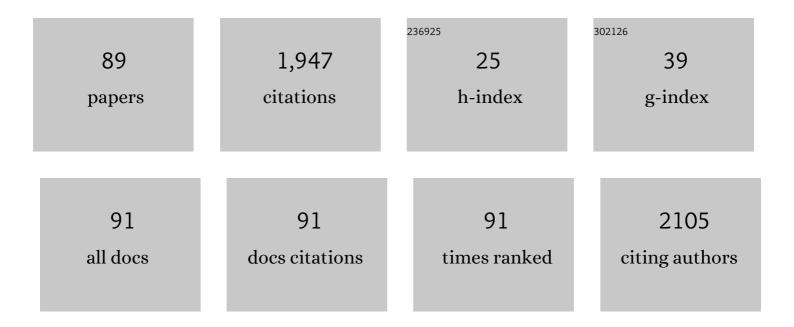
## GÃ;bor GalbÃ;cs

List of Publications by Year in descending order

Source: https://exaly.com/author-pdf/3257178/publications.pdf Version: 2024-02-01



CĂ:ROP CALRĂ:CS

#	Article	IF	CITATIONS
1	A critical review of recent progress in analytical laser-induced breakdown spectroscopy. Analytical and Bioanalytical Chemistry, 2015, 407, 7537-7562.	3.7	146
2	Methodology and applications of elemental mapping by laser induced breakdown spectroscopy. Analytica Chimica Acta, 2021, 1147, 72-98.	5.4	92
3	Recyclable ligand-free mesoporous heterogeneous Pd catalysts for Heck coupling. Tetrahedron Letters, 2005, 46, 7725-7728.	1.4	82
4	Laser-assisted metal deposition from liquid-phase precursors on polymers. Applied Surface Science, 2001, 172, 178-189.	6.1	78
5	Structural properties and photocatalytic behaviour of phosphate-modified nanocrystalline titania films. Applied Catalysis B: Environmental, 2007, 77, 175-183.	20.2	67
6	Semi-quantitative analysis of binary alloys using laser-induced breakdown spectroscopy and a new calibration approach based on linear correlation. Spectrochimica Acta, Part B: Atomic Spectroscopy, 2001, 56, 1159-1173.	2.9	62
7	Magnetic iron oxide/clay composites: effect of the layer silicate support on the microstructure and phase formation of magnetic nanoparticles. Nanotechnology, 2007, 18, 285602.	2.6	55
8	A Review of Applications and Experimental Improvements Related to Diode Laser Atomic Spectroscopy. Applied Spectroscopy Reviews, 2006, 41, 259-303.	6.7	49
9	A time-resolved imaging and electrical study on a high current atmospheric pressure spark discharge. Journal of Applied Physics, 2015, 118, .	2.5	48
10	Mechanical and chemical breaking of multiwalled carbon nanotubes. Catalysis Today, 2002, 76, 3-10.	4.4	47
11	Accurate quantitative analysis of gold alloys using multi-pulse laser induced breakdown spectroscopy and a correlation-based calibration method. Spectrochimica Acta, Part B: Atomic Spectroscopy, 2008, 63, 591-597.	2.9	47
12	Use of the Ar2+signal as a diagnostic tool in solid sampling electrothermal vaporization inductively coupled plasma mass spectrometry. Journal of Analytical Atomic Spectrometry, 1995, 10, 1047-1052.	3.0	44
13	Multi-pulse laser-induced plasma spectroscopy using a single laser source and a compact spectrometer. Journal of Analytical Atomic Spectrometry, 2005, 20, 974.	3.0	42
14	Niosomes decorated with dual ligands targeting brain endothelial transporters increase cargo penetration across the blood-brain barrier. European Journal of Pharmaceutical Sciences, 2018, 123, 228-240.	4.0	38
15	An Assessment of the Potential of Laser-Induced Breakdown Spectroscopy (LIBS) for the Analysis of Cesium in Liquid Samples of Biological Origin. Applied Spectroscopy, 2014, 68, 789-793.	2.2	36
16	Reaction dynamics of CW Ar+ laser induced copper direct writing from liquid electrolyte on polyimide substrates. Applied Surface Science, 2000, 158, 127-133.	6.1	33
17	Chloroplastic glutamine synthetase is activated by direct binding of aluminium. Physiologia Plantarum, 2009, 135, 43-50.	5.2	30
18	A Study of Ablation, Spatial, and Temporal Characteristics of Laser-Induced Plasmas Generated by Multiple Collinear Pulses. Applied Spectroscopy, 2010, 64, 161-172.	2.2	30

#	Article	IF	CITATIONS
19	On the applicability and performance of the single particle ICP-MS nano-dispersion characterization method in cases complicated by spectral interferences. Journal of Analytical Atomic Spectrometry, 2016, 31, 1112-1122.	3.0	29
20	Magnetic Phase Transition in Spark-Produced Ternary LaFeSi Nanoalloys. ACS Applied Materials & Interfaces, 2018, 10, 6073-6078.	8.0	29
21	An evaluation of the analytical performance of collinear multi-pulse laser induced breakdown spectroscopy. Microchemical Journal, 2011, 97, 255-263.	4.5	28
22	Discrimination of paper and print types based on their laser induced breakdown spectra. Spectrochimica Acta, Part B: Atomic Spectroscopy, 2014, 94-95, 48-57.	2.9	28
23	Determination of the structure and composition of Au-Ag bimetallic spherical nanoparticles using single particle ICP-MS measurements performed with normal and high temporal resolution. Talanta, 2018, 179, 193-199.	5.5	28
24	Cadmium Ion Adsorption Controls the Growth of CdS Nanoparticles on Layered Montmorillonite and Calumit Surfaces. Journal of Colloid and Interface Science, 1999, 213, 584-591.	9.4	27
25	Nanoparticle enhanced laser induced breakdown spectroscopy of liquid samples by using modified surface-enhanced Raman scattering substrates. Spectrochimica Acta, Part B: Atomic Spectroscopy, 2020, 166, 105793.	2.9	26
26	Solid sampling electrothermal vaporization inductively coupled plasma atomic emission spectrometry (ETV-ICP-AES): influence of some ICP operating param. Spectrochimica Acta, Part B: Atomic Spectroscopy, 1993, 48, 671-680.	2.9	25
27	Preparation and structural characterization of [Ph3Sn(IV)]+ complexes with pyridine-carboxylic acids or hydroxypyridine, -pyrimidine and -quinoline. Journal of Organometallic Chemistry, 2006, 691, 1622-1630.	1.8	25
28	A pH-Metric, UV, NMR, and X-ray Crystallographic Study on Arsenous Acid Reacting with Dithioerythritol. Inorganic Chemistry, 2008, 47, 3832-3840.	4.0	24
29	Dimensional characterization of gold nanorods by combining millisecond and microsecond temporal resolution single particle ICP-MS measurements. Journal of Analytical Atomic Spectrometry, 2017, 32, 2455-2462.	3.0	24
30	Effects of Continuous Low-Dose Exposure to Organic and Inorganic Mercury During Development on Epileptogenicity in Rats. NeuroToxicology, 2002, 23, 197-206.	3.0	23
31	Determination of the platinum concentration of a Pt/silica nanocomposite decorated with ultra small Pt nanoparticles using single particle inductively coupled plasma mass spectrometry. Journal of Analytical Atomic Spectrometry, 2017, 32, 996-1003.	3.0	21
32	From plasma to nanoparticles: optical and particle emission of a spark discharge generator. Nanotechnology, 2017, 28, 475603.	2.6	21
33	Nanoparticles in analytical laser and plasma spectroscopy – a review of recent developments in methodology and applications. Journal of Analytical Atomic Spectrometry, 2021, 36, 1826-1872.	3.0	20
34	Classification of minerals and the assessment of lithium and beryllium content in granitoid rocks by laser-induced breakdown spectroscopy. Journal of Analytical Atomic Spectrometry, 2021, 36, 813-823.	3.0	20
35	The Effect of Cadmium Ion Adsorption on the Growth of CdS Nanoparticles at Colloidal Silica Particle Interfaces in Binary Liquids. Journal of Colloid and Interface Science, 1997, 195, 307-315.	9.4	19
36	Mass spectrometric studies of thermal decomposition products of reference materials for use in solid sampling atomic spectrometry. Spectrochimica Acta, Part B: Atomic Spectroscopy, 1998, 53, 1335-1346.	2.9	19

#	Article	IF	CITATIONS
37	Characterization of a copper spark discharge plasma in argon atmosphere used for nanoparticle generation. Plasma Sources Science and Technology, 2017, 26, 045001.	3.1	19
38	Thermo-optical properties of residential coals and combustion aerosols. Atmospheric Environment, 2018, 178, 118-128.	4.1	19
39	Full range tuning of the composition of Au/Ag binary nanoparticles by spark discharge generation. Scientific Reports, 2021, 11, 5117.	3.3	19
40	A study of stalagmite samples from Baradla Cave (Hungary) by laser induced plasma spectrometry with automatic signal correction. Microchemical Journal, 2011, 99, 406-414.	4.5	18
41	Qualitative discrimination of coal aerosols by using the statistical evaluation of laser-induced breakdown spectroscopy data. Spectrochimica Acta, Part B: Atomic Spectroscopy, 2019, 153, 34-41.	2.9	18
42	Porosity determination of nano- and sub-micron particles by single particle inductively coupled plasma mass spectrometry. Journal of Analytical Atomic Spectrometry, 2020, 35, 1139-1147.	3.0	18
43	Determination of Cadmium in Certified Reference Materials Using Solid Sampling Electrothermal Vaporization Inductively Coupled Plasma Mass Spectrometry Supplemented with Thermogravimetric Studies. Microchemical Journal, 1996, 54, 272-286.	4.5	17
44	The effect of circuit resistance on the particle output of a spark discharge nanoparticle generator. Journal of Aerosol Science, 2018, 118, 59-63.	3.8	17
45	Oxidation of hydrocarbons by O2 in the presence of VO(acac)2 as catalyst. Journal of Molecular Catalysis A, 2002, 179, 65-72.	4.8	15
46	Optimization of plasma sampling depth and aerosol gas flow rates for single particle inductively coupled plasma mass spectrometry analysis. Talanta, 2017, 172, 147-154.	5.5	15
47	Facile and versatile substrate fabrication for surface enhanced Raman spectroscopy using spark discharge generation of Au/Ag nanoparticles. Applied Surface Science, 2020, 531, 147268.	6.1	15
48	An in vitro study of interactions between insulin-mimetic zinc(II) complexes and selected plasma components. Journal of Inorganic Biochemistry, 2006, 100, 1936-1945.	3.5	14
49	Qualitative Discrimination Analysis of Coals Based on Their Laser-Induced Breakdown Spectra. Energy & Fuels, 2016, 30, 10306-10313.	5.1	14
50	Slurry nebulization ICP-AES spectrometry method for the determination of tin in organotin(IV) complexes. Talanta, 2000, 52, 1061-1067.	5.5	13
51	Generalization of a new calibration method based on linear correlation. Talanta, 2004, 63, 351-357.	5.5	13
52	Observation of fine-ordered patterns on electrode surfaces subjected to extensive erosion in a spark discharge. Journal of Aerosol Science, 2016, 93, 16-20.	3.8	13
53	Gold Size Effect in the Thermal-Induced Reaction of CO <sub>2</sub> and H <sub>2</sub> on Titania- and Titanate Nanotube-Supported Gold Catalysts. Journal of Nanoscience and Nanotechnology, 2019, 19, 470-477.	0.9	13
54	Analysis and discrimination of soldering tin samples by collinear multi-pulse laser induced breakdown spectrometry, supported by inductively coupled plasma optical emission and mass spectrometry. Microchemical Journal, 2013, 107, 17-24.	4.5	12

#	Article	IF	CITATIONS
55	Silica-Based Catalyst Supports Are Inert, Are They Not?: Striking Differences in Ethanol Decomposition Reaction Originated from Meso- and Surface-Fine-Structure Evidenced by Small-Angle X-ray Scattering. Journal of Physical Chemistry C, 2017, 121, 5130-5136.	3.1	12
56	Surface features and energy considerations related to the erosion processes of Cu and Ni electrodes in a spark discharge nanoparticle generator. Journal of Aerosol Science, 2018, 119, 51-61.	3.8	12
57	Assessment and application of diode laser induced fluorescence spectrometry in an inductively coupled plasma to the determination of lithium. Spectrochimica Acta, Part B: Atomic Spectroscopy, 2005, 60, 299-306.	2.9	11
58	Investigation of the catalytic behavior of ion-pair complexes of vanadium(V) in the liquid-phase oxidation of hydrocarbons with molecular O2. Journal of Molecular Catalysis A, 2000, 164, 109-124.	4.8	10
59	Measurement and Modeling of Ozone and Nitrogen Oxides Produced by Laser Breakdown in Oxygen—Nitrogen Atmospheres. Applied Spectroscopy, 2003, 57, 1442-1450.	2.2	9
60	The feasibility of liquid sample microanalysis using polydimethylsiloxane microfluidic chips with in-channel and in-port laser-induced breakdown spectroscopy detection. Spectrochimica Acta, Part B: Atomic Spectroscopy, 2016, 126, 23-30.	2.9	9
61	Analysis and Classification of Liquid Samples Using Spatial Heterodyne Raman Spectroscopy. Applied Spectroscopy, 2019, 73, 1409-1419.	2.2	9
62	Synthesis and spectroscopic characterization of novel GFP chromophore analogues based on aminoimidazolone derivatives. Spectrochimica Acta - Part A: Molecular and Biomolecular Spectroscopy, 2019, 218, 161-170.	3.9	9
63	Synthesis and Fluorescence Mechanism of the Aminoimidazolone Analogues of the Green Fluorescent Protein: Towards Advanced Dyes with Enhanced Stokes Shift, Quantum Yield and Twoâ€Photon Absorption. European Journal of Organic Chemistry, 2021, 2021, 5649-5660.	2.4	9
64	X-ray Photoelectron Spectroscopic and Atomic Force Microscopic Studies of Pyrolytically Coated Graphite and Highly Oriented Pyrolytic Graphite Used for Electrothermal Vaporization. Journal of Analytical Atomic Spectrometry, 1997, 12, 951-955.	3.0	7
65	Construction and characterization of a diode laser system for atomic spectrometric experiments. Microchemical Journal, 2002, 73, 27-38.	4.5	7
66	Deuterium analysis by inductively coupled plasma mass spectrometry using polyatomic species: An experimental study supported by plasma chemistry modeling. Analytica Chimica Acta, 2020, 1104, 28-37.	5.4	7
67	Silybum marianum (milk thistle) products in Wilson's disease: a treatment or a threat?. Journal of Herbal Medicine, 2016, 6, 157-159.	2.0	6
68	Hg <sup>2+</sup> and Cd <sup>2+</sup> binding of a bioinspired hexapeptide with two cysteine units constructed as a minimalistic metal ion sensing fluorescent probe. Dalton Transactions, 2019, 48, 8327-8339.	3.3	6
69	Species-specific sensitivity of <i>Eisenia</i> earthworms towards noble metal nanoparticles: a multiparametric <i>in vitro</i> study. Environmental Science: Nano, 2020, 7, 3509-3525.	4.3	6
70	One-step fabrication of fiber optic SERS sensors via spark ablation. Nanotechnology, 2021, 32, 395501.	2.6	6
71	A Comprehensive Study of the Ca <sup>2+</sup> Ion Binding of Fluorescently Labelled BAPTA Analogues. European Journal of Organic Chemistry, 2021, 2021, 5248-5261.	2.4	6
72	A novel approach for discovering correlations between elemental and molecular composition using laser-based spectroscopic techniques. Analyst, The, 2022, 147, 3248-3257.	3.5	6

#	Article	IF	CITATIONS
73	The effect of sonication on glass electrodes. Talanta, 2005, 66, 809-812.	5.5	5
74	The activity of Au supported on various types of carbon in the ring transformation reactions of methyloxirane. Reaction Kinetics and Catalysis Letters, 2006, 87, 343-348.	0.6	5
75	Synthesis, structural characterisation, and catalytic activity of Mn(II)–protected amino acid complexes covalently immobilised on chloropropylated silica gel. Catalysis Today, 2015, 241, 264-269.	4.4	5
76	Designed Pt Promoted 3D Mesoporous Co3O4 Catalyst in CO2 Hydrogenation. Journal of Nanoscience and Nanotechnology, 2019, 19, 436-441.	0.9	5
77	Modulation of the catalytic activity of a metallonuclease by tagging with oligohistidine. Journal of Inorganic Biochemistry, 2020, 206, 111013.	3.5	5
78	Qualitative Analysis of Glass Microfragments Using the Combination of Laser-Induced Breakdown Spectroscopy and Refractive Index Data. Sensors, 2022, 22, 3045.	3.8	5
79	Laser-induced breakdown spectroscopy signal enhancement effect for argon caused by the presence of gold nanoparticles. Spectrochimica Acta, Part B: Atomic Spectroscopy, 2022, 193, 106435.	2.9	5
80	Multifunctional microfluidic chips for the single particle inductively coupled plasma mass spectrometry analysis of inorganic nanoparticles. Lab on A Chip, 2022, 22, 2766-2776.	6.0	4
81	Cd(II) Capture Ability of an Immobilized, Fluorescent Hexapeptide. Bulletin of the Chemical Society of Japan, 2016, 89, 243-253.	3.2	3
82	Optical modeling of the characteristics of dual reflective grating spatial heterodyne spectrometers for use in laser-induced breakdown spectroscopy. Spectrochimica Acta, Part B: Atomic Spectroscopy, 2021, 183, 106236.	2.9	3
83	Slurry nebulization ICP-AES spectrometry method for the determination of tin in organotin(IV) complexes. Talanta, 2000, 52, 1061-7.	5.5	3
84	Protective effect of green tea against neuro-functional alterations in rats treated with MnO2nanoparticles. Journal of the Science of Food and Agriculture, 2017, 97, 1717-1724.	3.5	2
85	Size-Dependent H <sub>2</sub> Sensing Over Supported Pt Nanoparticles. Journal of Nanoscience and Nanotechnology, 2019, 19, 459-464.	0.9	2
86	Response to the comments. Spectrochimica Acta, Part B: Atomic Spectroscopy, 2009, 64, 359-360.	2.9	0
87	Partial mummification and extraordinary context observed in perinate burials: a complex osteoarcheological study applying ICP-AES, μXRF, and macromorphological methods. Archaeological and Anthropological Sciences, 2018, 10, 685-695.	1.8	0
88	Egy- és többkomponensű plazmonikus nanorészecskék szikra-plazma alapú előállÃŧása és alkalma felületerÅ'sÃŧett Raman spektroszkópiában. , 2021, , .	azÃ;suk a	0
89	Milk thistle in Wilson's disease: what is the pledge of safety?. Planta Medica, 2015, 81, .	1.3	0